Supplementary information

for

Anthropogenic aerosols delay the emergence of GHGs-forced wetting of South Asian rainy seasons under a fossil-fuel intensive pathway

Jitendra Singh[1,2*], Benjamin I. Cook[3,4], Kate Marvel[3,5], Sonali McDermid[6], Geeta G. Persad[7], Bala Rajaratnam[8], Deepti Singh[2]

[1]Institute for Atmospheric and Climate, ETH Zurich, Switzerland
[2]School of the Environment, Washington State University, Vancouver, WA, USA
[3]NASA Goddard Institute for Space Studies, New York, NY, USA
[4]Lamont-Doherty Earth Observatory, Columbia University, Palisade, NY, USA
[5]Center for Climate Systems Research, Columbia University, New York, NY, USA
[6]Department of Environmental Studies, New York University, New York, NY, USA
[7]Department of Geological Sciences, University of Texas at Austin, Texas, USA
[8]Department of Statistics, University of California, Davis, Davis, California, USA

[*]Corresponding author: jitendra.singh@env.ethz.ch

Content of this file

Figures S1 to S10

Supplementary Figures

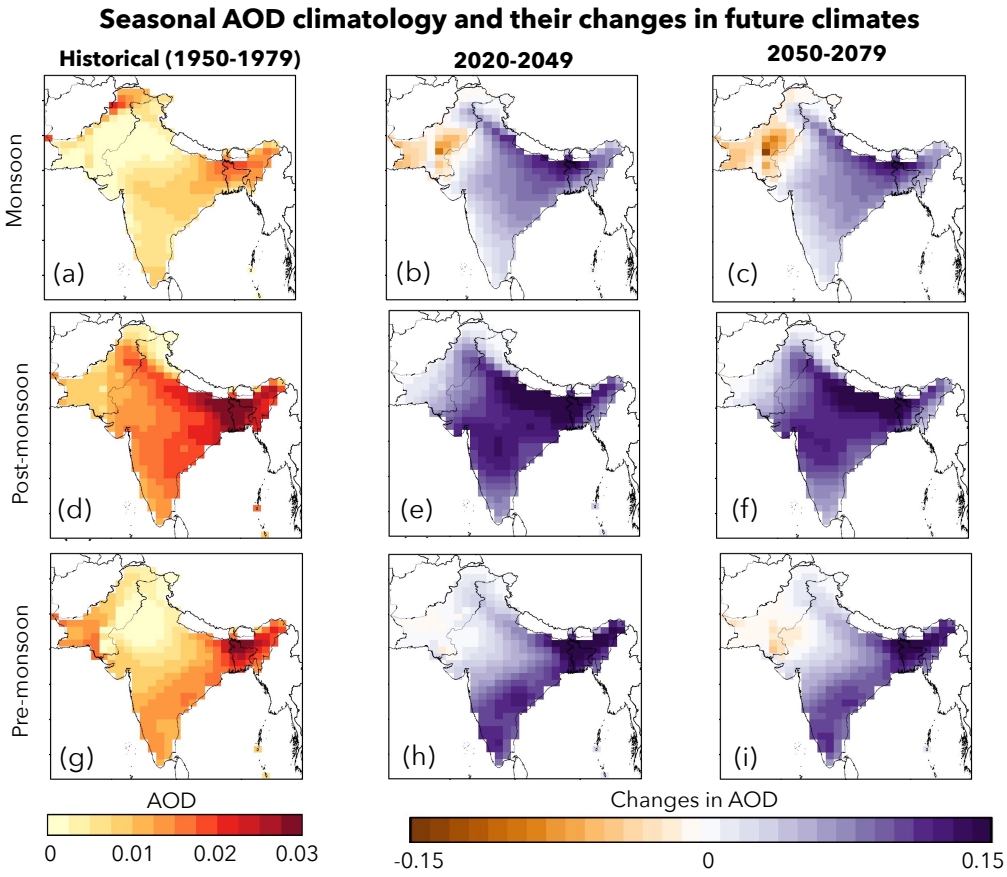

Figure S1. Seasonal aerosol optical depth (AOD) climatology and their changes in the mid- (2020-2049) and late-21st century (2050-2079) in response to AAER. c

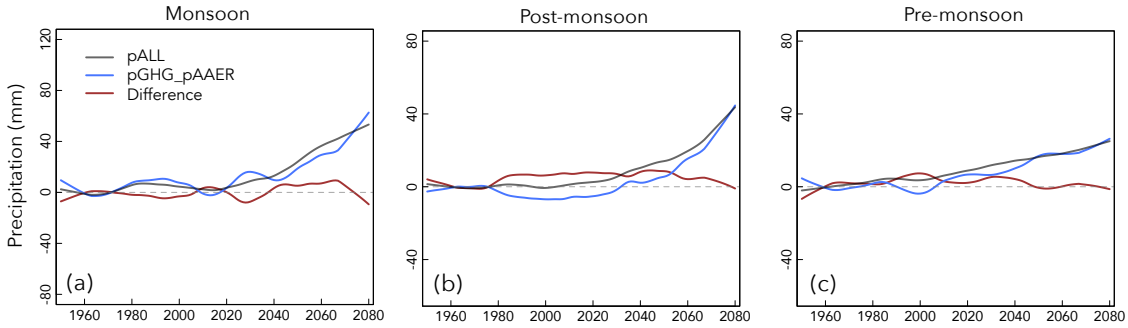

Figure S2. Comparison of seasonal precipitation response to ALL-forcing (black line) and the sum of GHGs and AAER-forced precipitation ($P_{GHG} + P_{AAER}$; blue line) over South Asia. Red line indicates the precipitation difference between ALL-forcing and the sum of GHGs and AER precipitation.

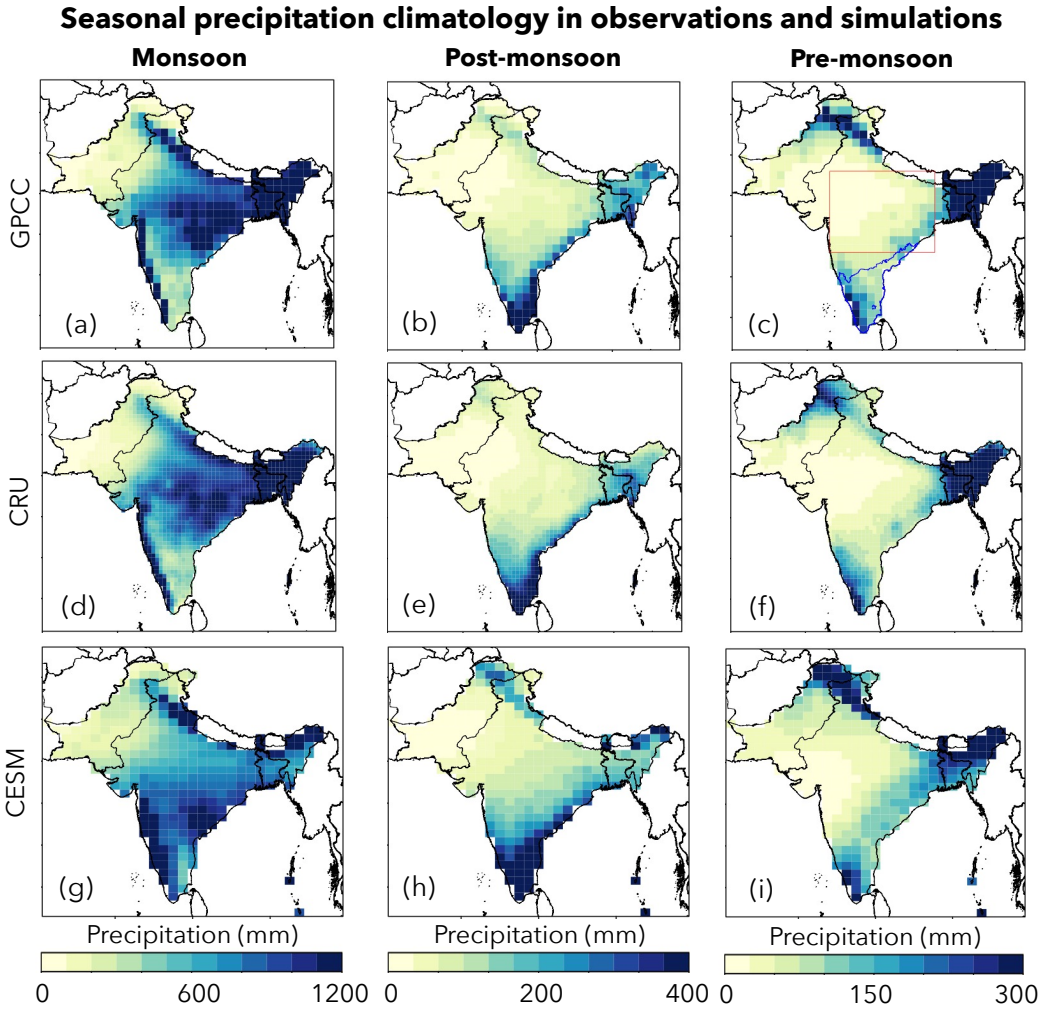

Figure S3: Historical precipitation in observations (CRU and GPCC) and simulations (CESM1-LE ALL). Red box in (c) indicate the North Central India (NCI) domain.

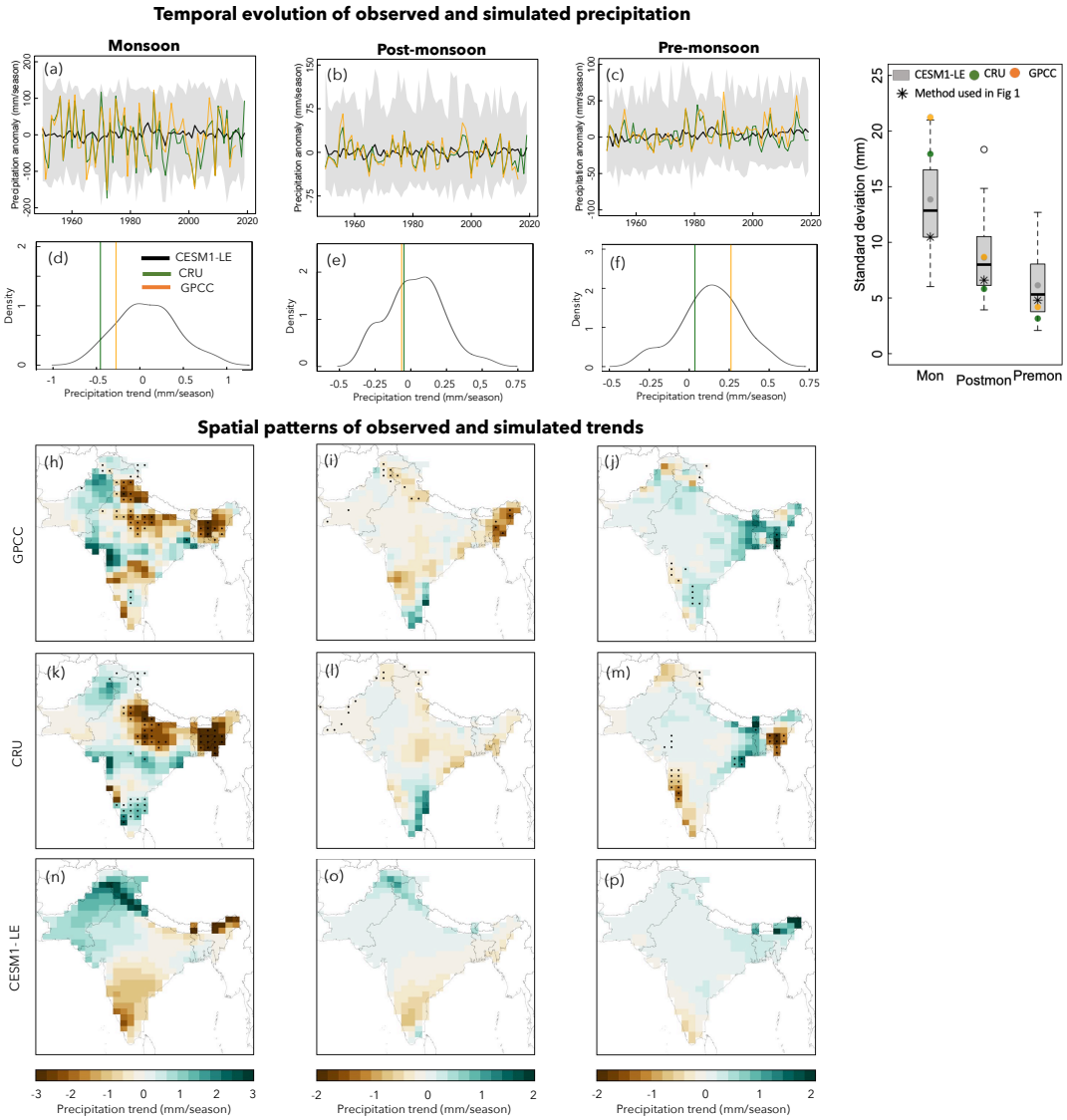

Figure S4. (**a-c**) The observed and simulated time series of regional averaged seasonal precipitation changes relative to 1950-1979 over South Asia. Grey shaded indicate the spread of CESM1-LE (min-to-max across the ensemble). (**d-f**) Comparison of simulated and observed trends in regional averaged seasonal precipitation for CESM1-LE, CRU and GPCC (1950-2016). (**d**) Seasonal precipitation variability (standard deviation) in 10-year running means of individual ensemble members (boxplots), CRU (green dot) and GPCC (orange dot), and the ensemble mean precipitation (asterisk symbol). **(h-p)** Spatial patterns of simulated and observed trends in seasonal precipitation. Grid cells with dots represent areas where observed trends fall outside the range of CESM1-LE. The lower panels show the average trend in CESM1-LE.

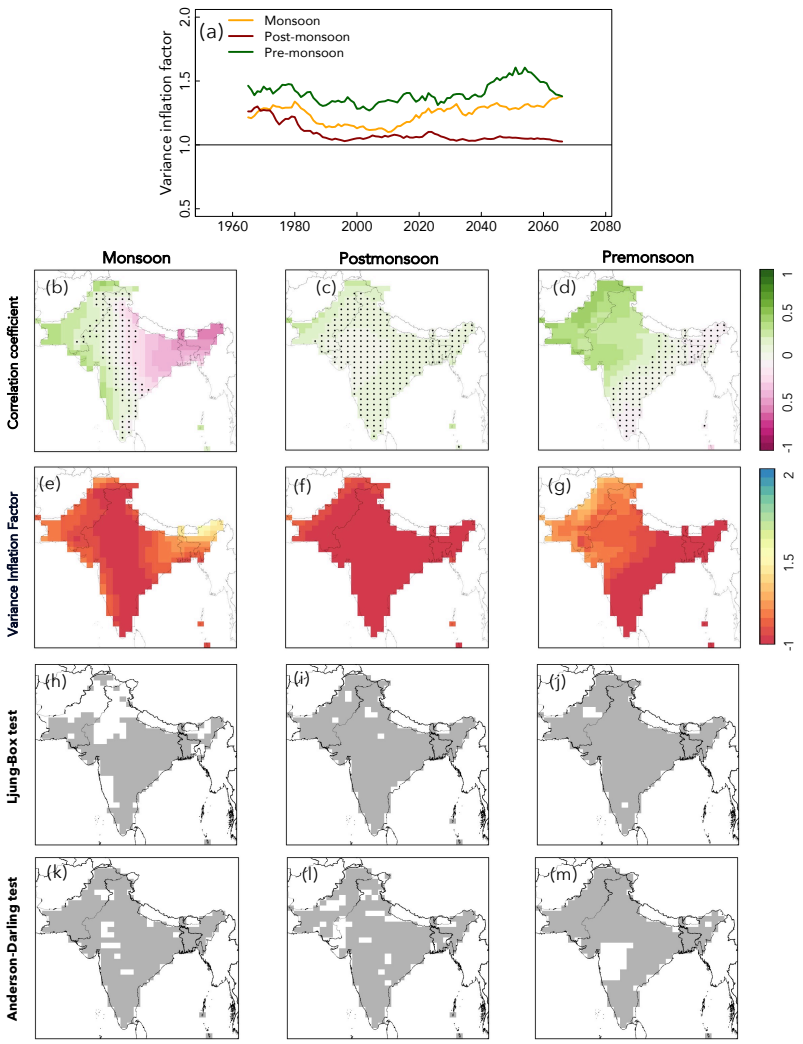

Figure S5. (a) Variance inflation factor of regression models used in regional-average analysis (presented in Fig 3d-f) in all seasons **(b-d)** Correlation between local and remote aerosols in monsoon, post-monsoon, and pre-monsoon seasons. Dots indicate the grid cells with insignificant correlation. **(e-g)** variance inflation factor from regression models (1950-2049) used at each grid cells in all seasons. **(h-j)** Analysis of residuals from the multiple linear regression. **(g-i)** Grey color indicates the grid cells where residual from multiple linear regression model is independent (based on Ljung-Box test at 5% significance level). **(k-m)** Grey color indicates that the residuals at the corresponding grid cells follow the standard normal distribution based on Anderson-Darling test (5% significance level).

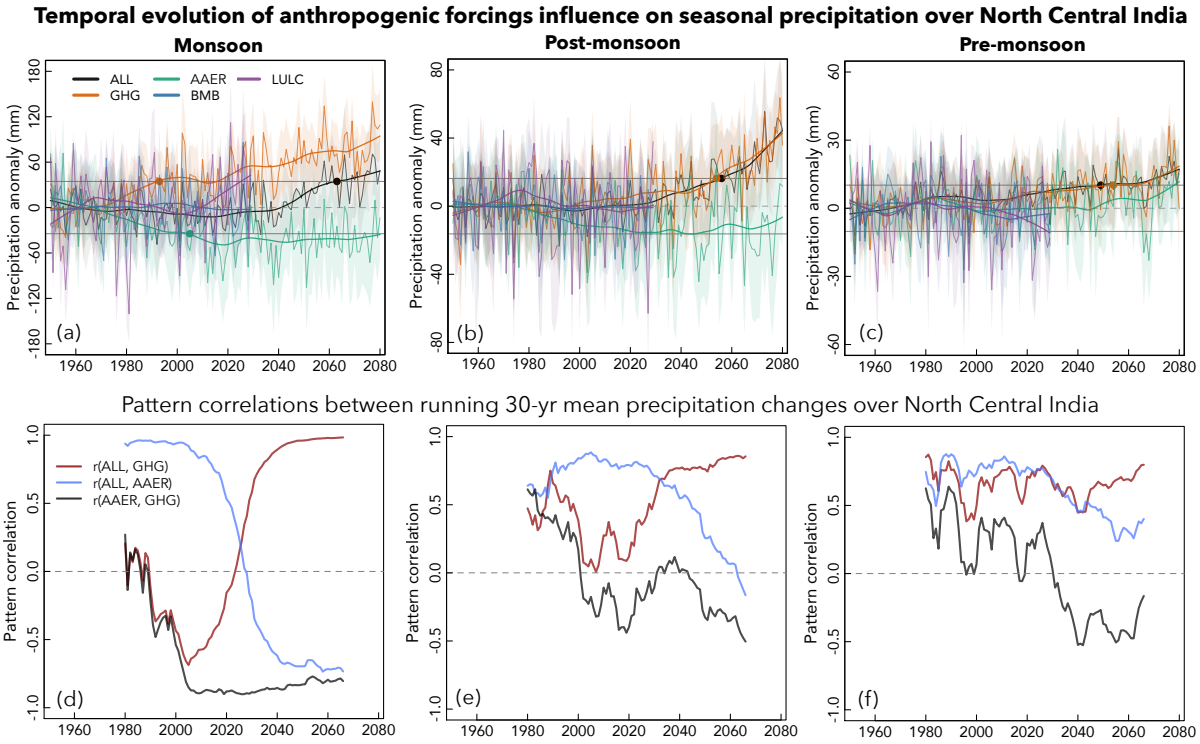

Figure S6. Same as Figure 1 but for North Central India.

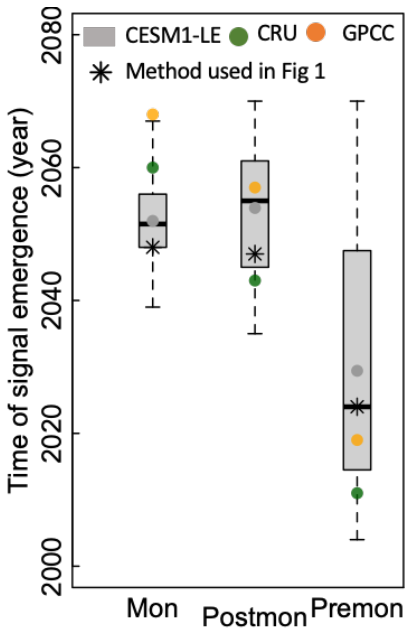

Figure S7. Sensitivity of the time of emergence of the precipitation signal in ALL-forcing simulations to definitions of noise. The boxplots present the distribution of the time of emergence based on noise derived from 10-year running mean precipitation in each individual ensemble member. The green and orange dots indicate the time of emergence based on noise from the 10-year running mean CRU and GPCC precipitation data, respectively. The asterisk indicates the time of emergence based on noise calculated from the ensemble mean precipitation (used in Figure 1).

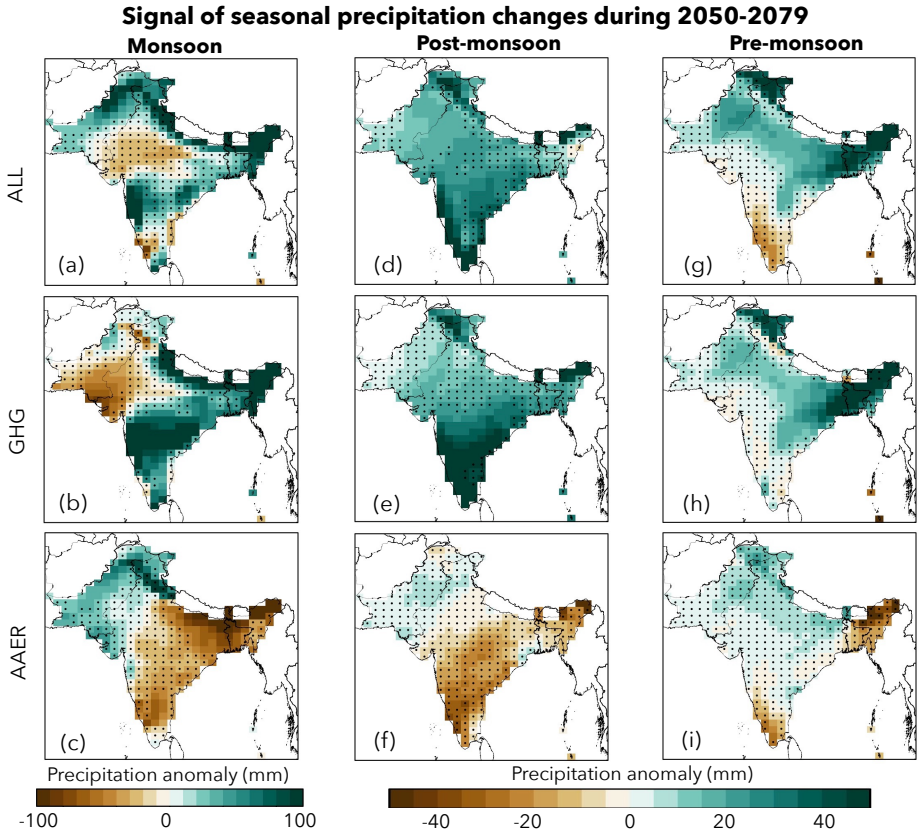

Figure S8. Signal-to-noise in seasonal precipitation changes. Ensemble-mean (a-c) monsoon, (d-f) post-monsoon and (g-i) pre-monsoon precipitation changes (signal) in ALL, GHG, and AER in the near-term (2050-2079) relative to climatological (1950-1979) period. Noise is defined as the 2 σ of precipitation changes across the ensemble members. Dots indicate the grid cells where the precipitation change does not exceed noise (signal-to-noise (S/N) $\leq$ 1). *See 'methods' for details.*

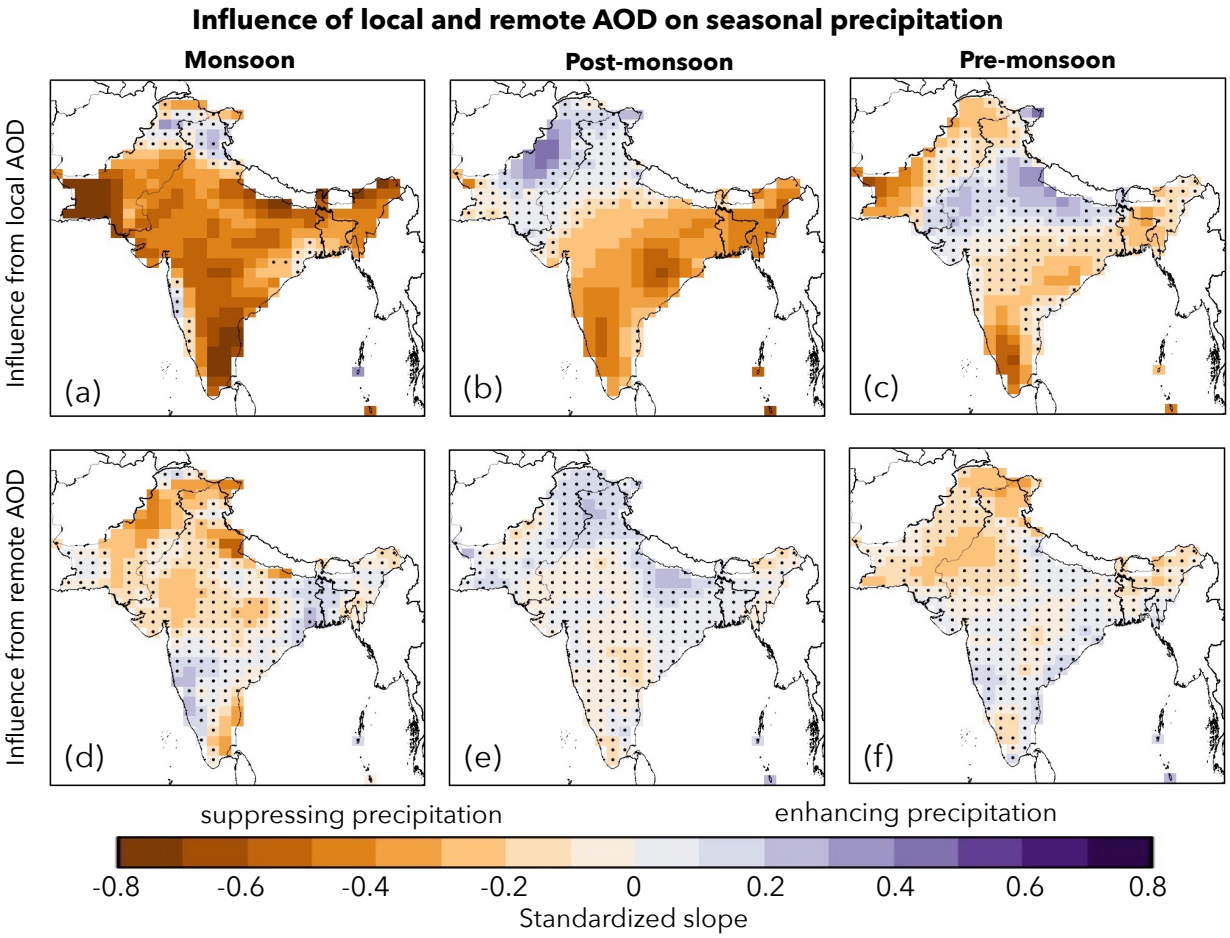

Figure S9. Influence of local and remote AOD on aerosols-driven seasonal precipitation. (a-c) Standardized slopes of local AOD based on multiple linear regression (*see "methods" for details*) of monsoon, post-monsoon and pre-monsoon season precipitation with local and remote AOD. (d-f) same as (a-c) but for remote AOD. Dots indicate the statistically insignificant (at 5% significance level) influence (slope value) from local/remote AOD on AAER-precipitation.

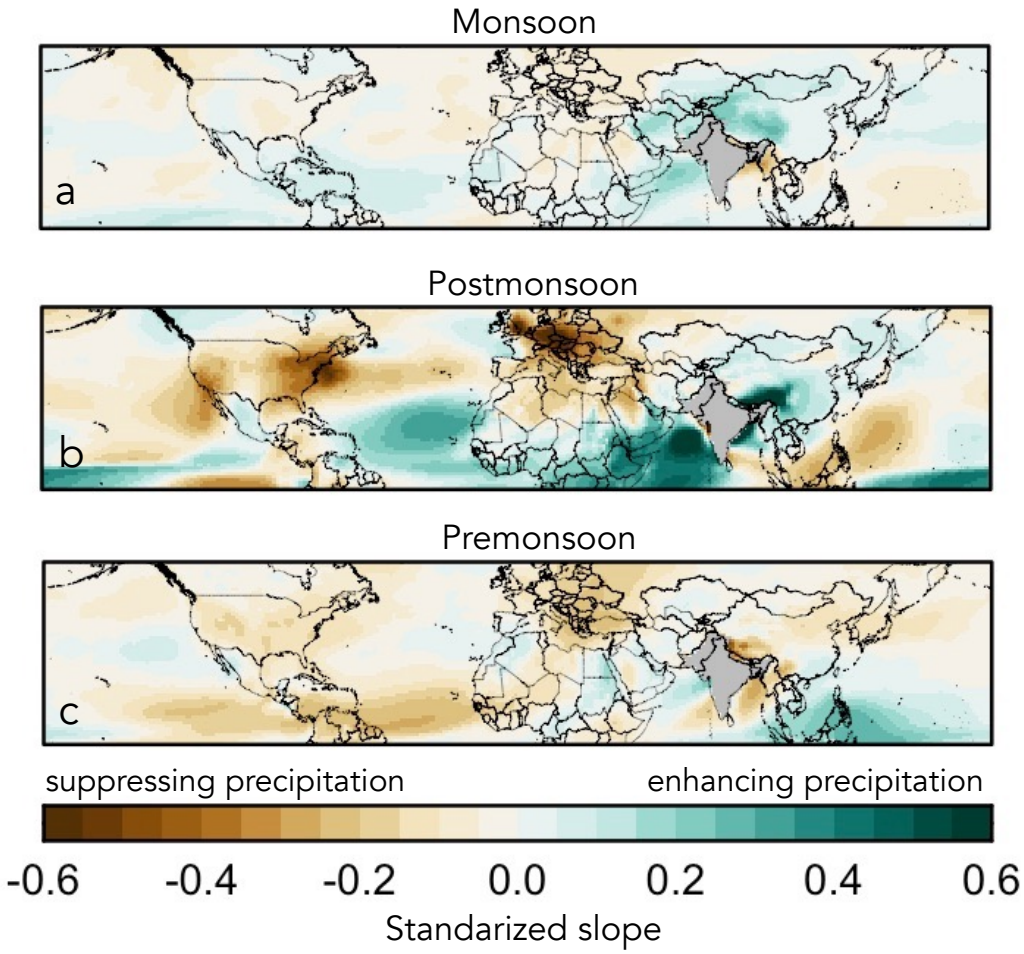

Figure S10: Location of remote aerosol influencing south Asian precipitation. Color represents regression coefficient of gridded remote (outside South Asia) aerosols obtained from a multiple linear regression (1950-2049) presented in Equation 2 in the main text.